Internal Report
DESY D3/34
May 1981

Some Measurements of Absorbed Dose due to Synchrotron Radiation in the PETRA Tunnel

by

H. Dinter and K. Tesch

Some measurements of absorbed dose due to synchrotron radiation in the PETRA tunnel

by

H. Dinter and K. Tesch

Summary: Absorbed doses measured with glass dosimeters inside the tunnel of the electron-storage-ring PETRA are reported. Also included are data on absorption of synchrotron radiation, effective energies, the dependance on beam energy and on the effect of the lead shield of the accelerator.

1. Introduction

Synchrotron radiation may cause severe problems at high-energy electron ring accelerators. High absorbed doses lead to damages in sensitive accelerator components, e.g. magnet coil insulation, cables, water hoses, electronic devices, and scattered synchrotron radiation may cause background problems for the experiments. We started our dose measurements in the PETRA tunnel when a beam energy of 13 GeV had been reached. At that time the vacuum pipe between the magnets and also the long straight sections near to the experimental halls were not covered with lead. The purpose of these measurements was to assist the machine groups in reducing the radiation background. At a beam energy of 15 GeV radiation damages became serious, and the whole vacuum pipe including all straight sections were shielded with 3 mm of lead. We extended the dose measurements to 17 GeV; the results at this energy, obtained under well-defined machine conditions, are intended for a comparison with Monte-Carlo calculations.

2. The measurements

The measurements reported in this paper were performed in the PETRA tunnel near the position SOL 125 (see Fig. 1) in the bow between hall SO and hall O, and at a long straight section near hall NO (location NOR 25).

To measure absorbed doses we used silver-activated phosphate glass dosimeters, 1 mm Ø x 6 mm, covered with 1 to 2 mm of plastics. The mass-energy-absorption coefficient of this glass is very similar to that of aluminium (fig. 2). Therefore we regard the dose measured in glass as a dose absorbed in a typical accelerator structure.

For measuring absorbed doses the radiation equilibrium between primary photons and secondary electrons should be established at the position of the dosimeter. Then the kerma inside the dosimeter (which can be calculated from the incoming photon fluence) equals the measured energy deposited in the glass. For the dosimeter actually used deviations from radiation equilibrium are expected at the high-energy end of the synchrotron radiation spectrum (0.1 to 1 MeV) because of escaping Compton electrons. Simple

measurements at 1.2 MeV show, however, that the difference between a dose measured at radiation equilibrium (glass dosimeter surrounded by 2 mm of aluminium) and a dose measured with the dosimeter mentioned above is less than 10%. At very low energies the radiation equilibrium can also not be established because of the absorption of the primary photons by the glass rod. But Monte-Carlo-calculations show that this effect is noticeable only at energies below 20 keV, and that in this energy range the contribution of photons to the dose outside the vacuum chamber of the accelerator is small*). Therefore we take our measurements to be measurements of absorbed dose or kerma in glass or aluminium.

Doses relevant for personal dosimetry should be measured with a material being more tissue-equivalent, e.g. by using LiF thermoluminescence dosimeters. We compared both methods at position NOR 25. At 17 GeV and with the long straight sections completely shielded with 3 mm of lead we found the ratios of the dose measured by glass dosimeters to the dose measured by LiF being 4.8 ± 0.5. With incomplete lead shielding the ratio was even higher, 10.2 ± 1.8, averaged over many positions across the tunnel. The reason is of course the strong contribution of photons of very low energies. To have a rough indication to the photon spectrum we measured the doses at the same position (and complete lead shielding) behind thin absorbers and calculated an effective photon energy from the doses before and behind a given absorber sheet. The results are given in table 1

Table 1

Doses measured between	Effective energy (keV)
0 and 1 mm Al	40
0 and 1 mm Cu	58
0 and 1 mm Pb	64
1 mm Cu and 2 mm Cu	75
2 mm Cu and 3 mm Cu	95
1 mm Pb and 2 mm Pb	160

*) Ch. Yamaguchi, DESY, forthcoming report

and are insensitive to the beam energy between 15 and 17.7 GeV because of multiple scattering in the tunnel. A complete absorption curve in lead and the corresponding effective energies are shown in fig. 3 (beam energy 17.7 GeV, vacuum chamber completely shielded with lead). For shielding estimates for a thin concrete wall an absorption coefficient of 0.050 cm^2/g (corresponding to 90 keV) is found to be appropriate.

In the following sections we give the results of a limited number of measurements which may be of general interest. The beam energy is 17 GeV unless otherwise stated. All doses are normalized to an integrated total current of 100 mA h. The mean currents both of electrons and positrons during the measurements were 5 to 10 mA, the ratio of electron beam to positron beam being 1.0 on the average.

3. Radiation doses in the gap of a dipole magnet

Doses absorbed in glass along the vacuum pipe before and behind its lead shield have been measured inside the gap of a dipole magnet at position SOL 125, inside and outside of the ring, see fig. 4. The data are given in table 2. They will be used for comparison with calculations because of the relatively simple geometry.

The dose distribution along the vacuum chamber is very uniform inside the ring (strings C and D in fig. 4) and also on the outside behind the lead shield (string A). A mean value for each of these cases is given in table 2. The distribution along string B is more complicated. The synchrotron radiation originating from the electron beam (going from left to right in the lower part of fig. 4) in one dipole magnet hits the inner surface of the vacuum pipe roughly between the end of this dipole and the middle of the next dipole. Therefore all our dosimeters of string B are covered with synchrotron radiation from electrons. The vacuum pipe of the straight section, however, is smaller than that inside a dipole magnet, and its lead shield shadows a few of the dosimeters next to the straight section. The synchrotron radiation of the positrons also hits the vacuum chamber up to the middle of the dipole magnet, and the last few dosimeters of string B could see also this component. Therefore the dose value resulting from both electron and positron synchrotron radiation, normalized to 100 mAh, is $4.8 \cdot 10^7$ rad.

Table 2

Doses in the gap of a dipole magnet

Z (cm)	A (10^3 rad)	B (10^7 rad)	Z (cm)	C (10^6 rad)	D (10^3 rad)
-15	7.2	0.16	104	1.8	7.2
-5	13.	0.41	122	1.4	7.8
5	14.	0.48	140	1.3	7.8
15	7.2	0.60	158	1.4	6.0
25	12.	0.41	176	1.3	6.0
35	9.0	0.49	194	1.6	4.8
45	5.4	0.96	212	2.2	5.7
55	9.0	0.72	230	1.3	5.8
65	5.4	0.72	248	1.6	7.2
75	6.6	0.96	266	2.4	5.8
85	7.2	1.0	284	1.0	5.7
95	7.2	1.8	302	1.8	7.2
105	7.2	1.6	320	1.4	6.6
115	8.4	2.6	338	1.1	6.6
125	6.6	2.4	356	1.3	5.0
135	7.8	2.4	374	1.8	6.6
145	6.0	2.5	392	1.1	7.2
155	7.2	4.2	410	1.6	8.4
165	7.2	4.3	418	1.6	7.2
175	9.0	5.1			
Average value	8.4±0.3	*		1.5±0.4	6.6±0.9

Z = Distance from the left edge of the dipole yoke.

* = see chap. 3

For positions A, B, C, D see fig. 4

4. Radiation doses in the tunnel near a dipole magnet

A series of dosimeters were distributed across the tunnel at position SOL 125 in a plane perpendicular to the beams near a short straight section between a dipole and a sextupole magnet (strings A, B and C, see figs. 5 and 6), the dose values are plotted in fig. 5. The resulting pattern is rather uniform due to many scattering processes of the photons; superimposed is an increase when approaching the vacuum pipe. The region around the vacuum pipe is of special interest, therefore the dosemeters were arranged in a smaller lattice there. A typical dose pattern is given in fig. 7, the values depend strongly on the special lead sheet arrangement around the vacuum chamber and bellows.

The radial dependence of the dose at nearly the same position (string D in fig. 6) was investigated in more detail; the results are shown in fig. 8. Within a distance of 1 m the doses obey roughly a 1/r-law (as one would expect), but beyond 1 m the distribution is rather flat due to multiple scattering along the tunnel.

The dependence in beam direction was studied with three strings of dosimeters (E, F and G in figs. 6 and 9), each 7 m long to cover the length of a cell of the magnet structure. The results are plotted in fig. 9. Again the distribution is rather uniform except near the section between the dipole and the sextupole magnet where the dose is governed by the irregularities of the lead shield.

The shielding of the short sections between the magnets is quite important. Omitting the 3 mm lead shield increases the doses in the tunnel regions mentioned above by a factor of 100; the doses at the front face of the magnet coils are increased by a factor between 100 and 1000 (measured at 15.5 GeV). The lead also reduces the energy dependence. Near an unshielded short straight section the doses rose by a factor of 10 when going from 14 to 16 GeV. Near a shielded section the factor is 2 to 5 for an increase in beam energy from 15 to 17 GeV.

5. Radiation doses in the straight tunnel part near a hall

In sections 3 and 4 dose values are reported which may be typical for the radiation field in the four bow parts of the tunnel. Other measurements were performed in a long straight tunnel section near an experimental hall, 15 m behind the last dipole magnet and 15 m before the next hall (position NOR 25).

On the average the absorbed doses in glass measured across the tunnel are only a factor 2 to 10 lower than in the curved tunnel section, provided that the long straight parts of the vacuum pipe are completely shielded with 3 mm of lead as well. Omitting this shield will rise the doses by a factor of 50 (at 15 GeV). The energy dependence is found to be the same as mentioned in section 4. The nearly uniform distribution across the tunnel is shown in fig. 10; the measurements are extended into a survey channel to study the attenuation of synchrotron radiation in a small duct. Even around the vacuum chamber the distribution is rather uniform; at the outside of the shielded long straight chamber the doses are only a factor 2 to 3 higher than at the inner side (nearer to the center). All these data support the picture of a relatively uniform radiation field along the PETRA tunnel for distances from the beam greater than 50 cm.

Figure captions

1. Part of the DESY site. Indicated are the two measuring positions SOL 125 and NOR 25 inside the PETRA tunnel.

2. Mass-energy-absorption coefficiens of dosimeter glass and aluminium.

3. Attenuation of scattered synchrotron radiation by lead and the corresponding effective energies, 1 m above beam at position NOR 25. Beam energy 17.7 GeV, vacuum pipe completely shielded with lead.

4. Positions of dosimeters and shielding materials inside the dipole magnet. Profile (above) and top view (below).

5. Absorbed doses across the tunnel. (Strings A,B,C, see also fig.6)

6. Positions of the strings of dosimeters (top view).
   A, B and C (see also fig. 5) perpendicular to the beams.
   D: in beam height. E: on top of the magnets.
   F: on the floor. G: at the wall in beam height.

7. Dose distribution near the vacuum chamber.

8. Radial dose distribution in beam height. (String D in fig. 6)

9. Dose distributions along the beams. (Strings E, F, G see also fig. 6)

10. Absorbed doses across the tunnel and in a survey channel at position NOR 25.

POSITIONS OF THE MEASUREMENTS

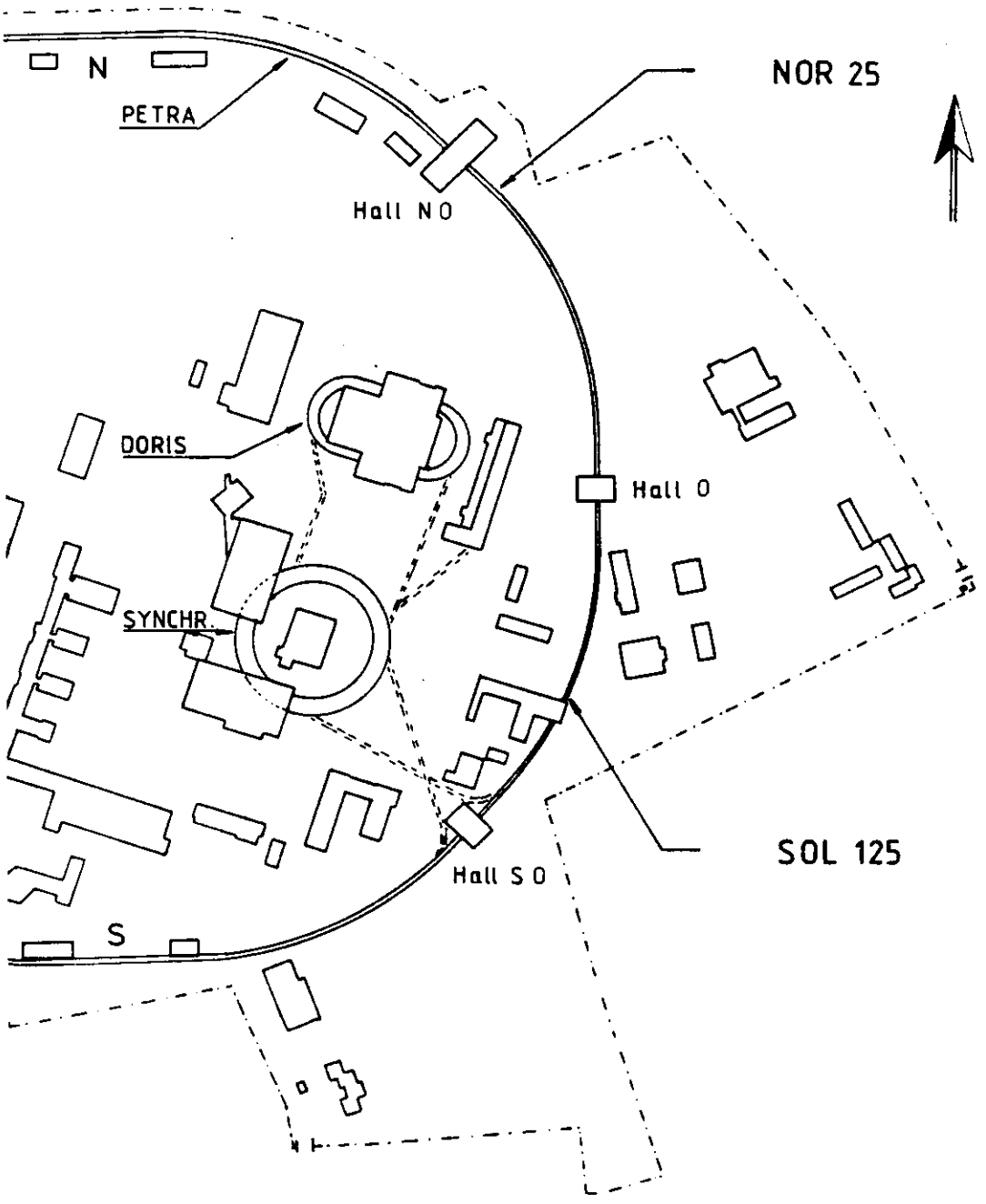

Fig.1

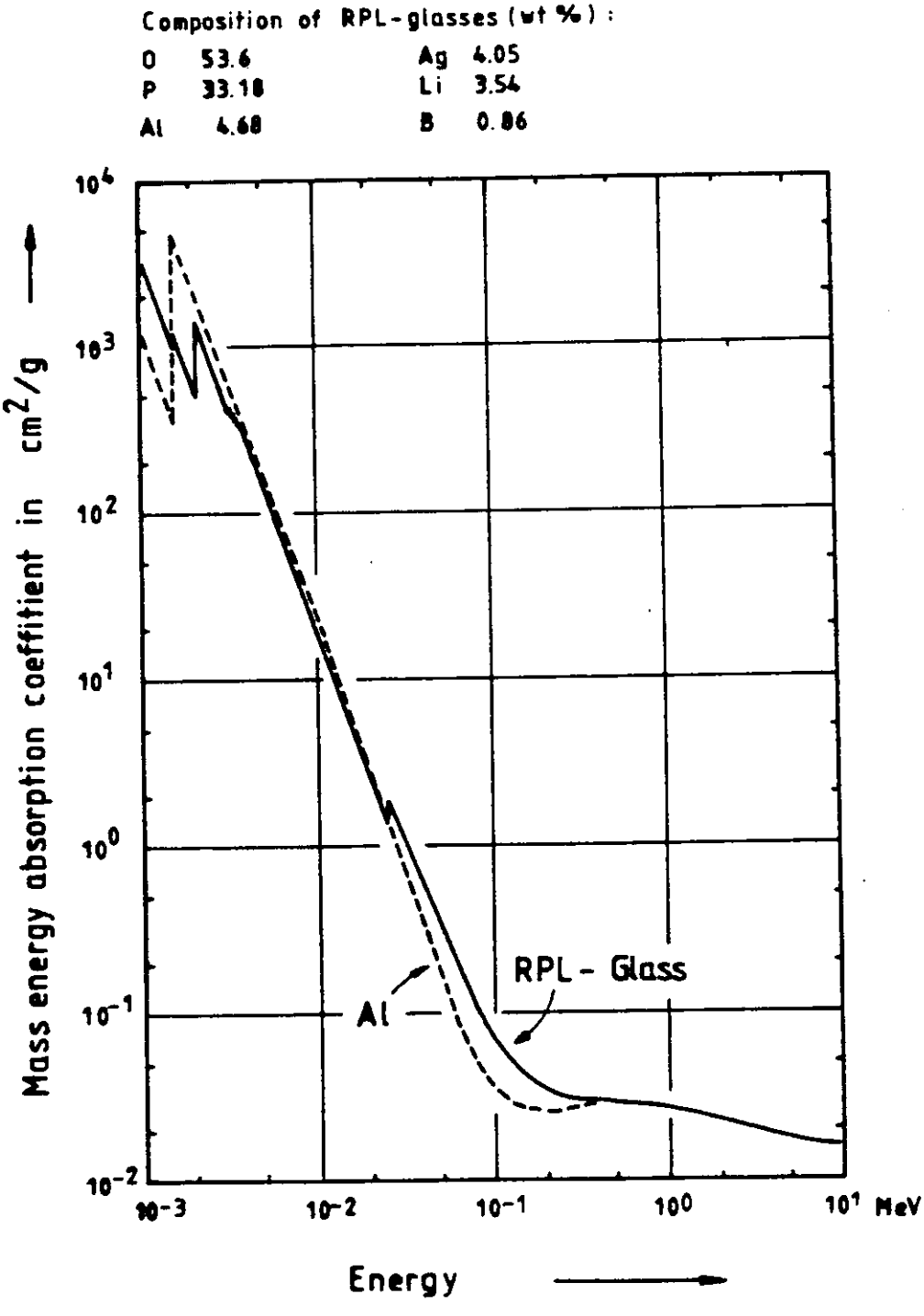
Composition of RPL-glasses (wt %) :
O 53.6
P 33.18
Al 4.68
Ag 4.05
Li 3.54
B 0.86
Mass energy absorption coeffitient in cm²/g
10⁴
10³
10²
10¹
10⁰
10⁻¹
10⁻²
10-3
10-2
10-1
10⁰
10¹ MeV
Energy
RPL - Glass
Al

Fig. 2

POS. NOR 25 1 metre above beam

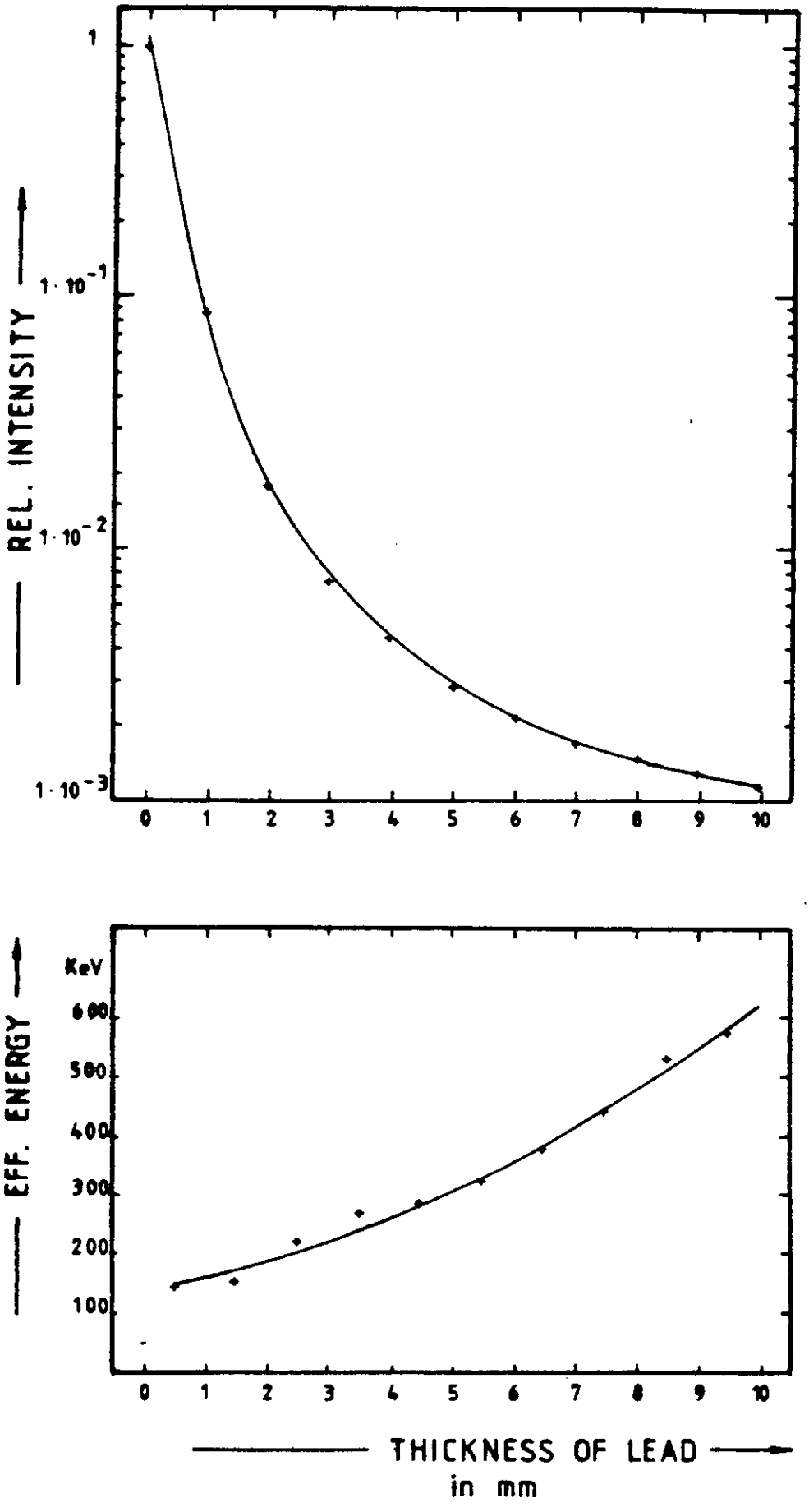

Fig. 3

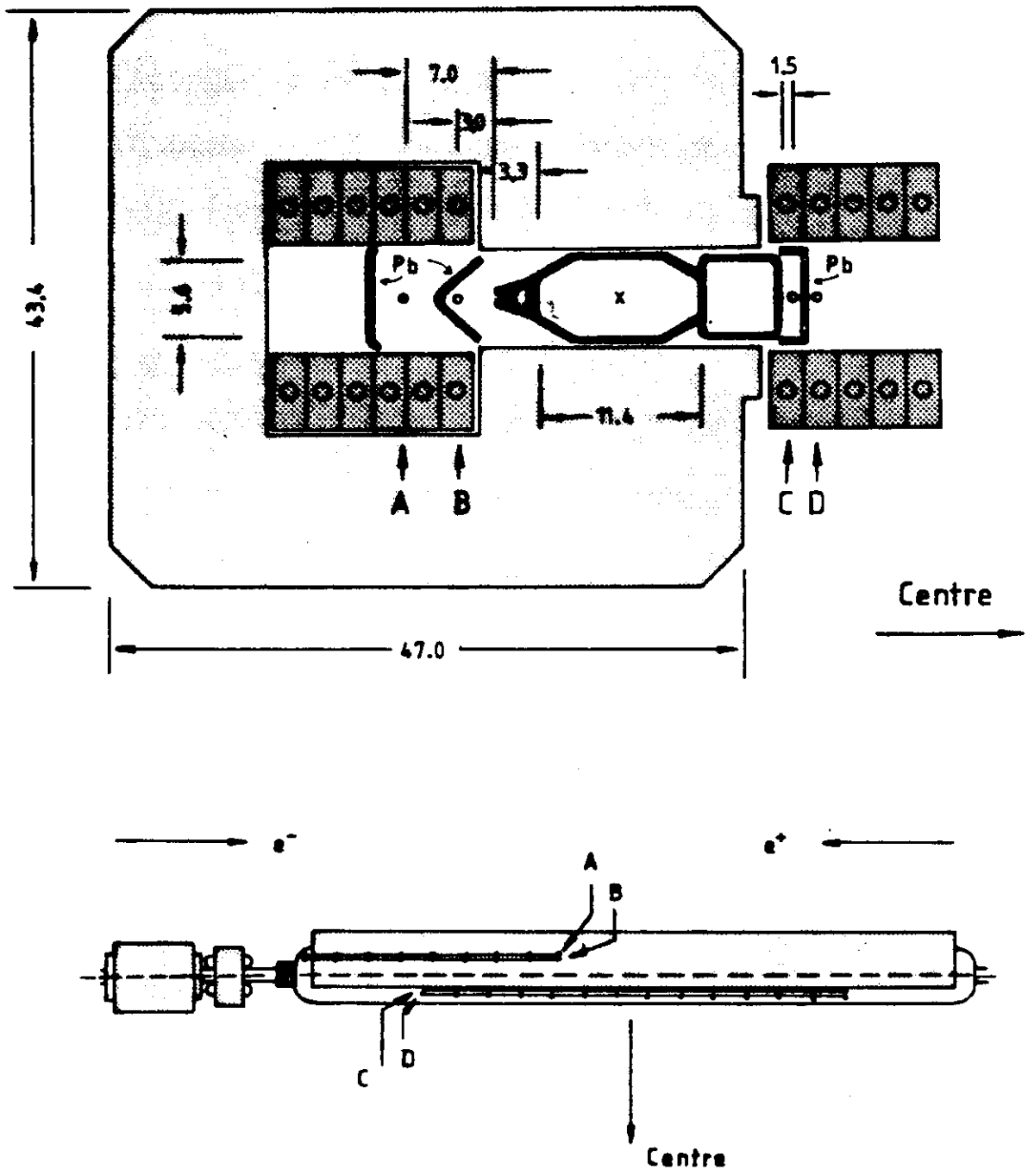

Units: cm

Fig. 4

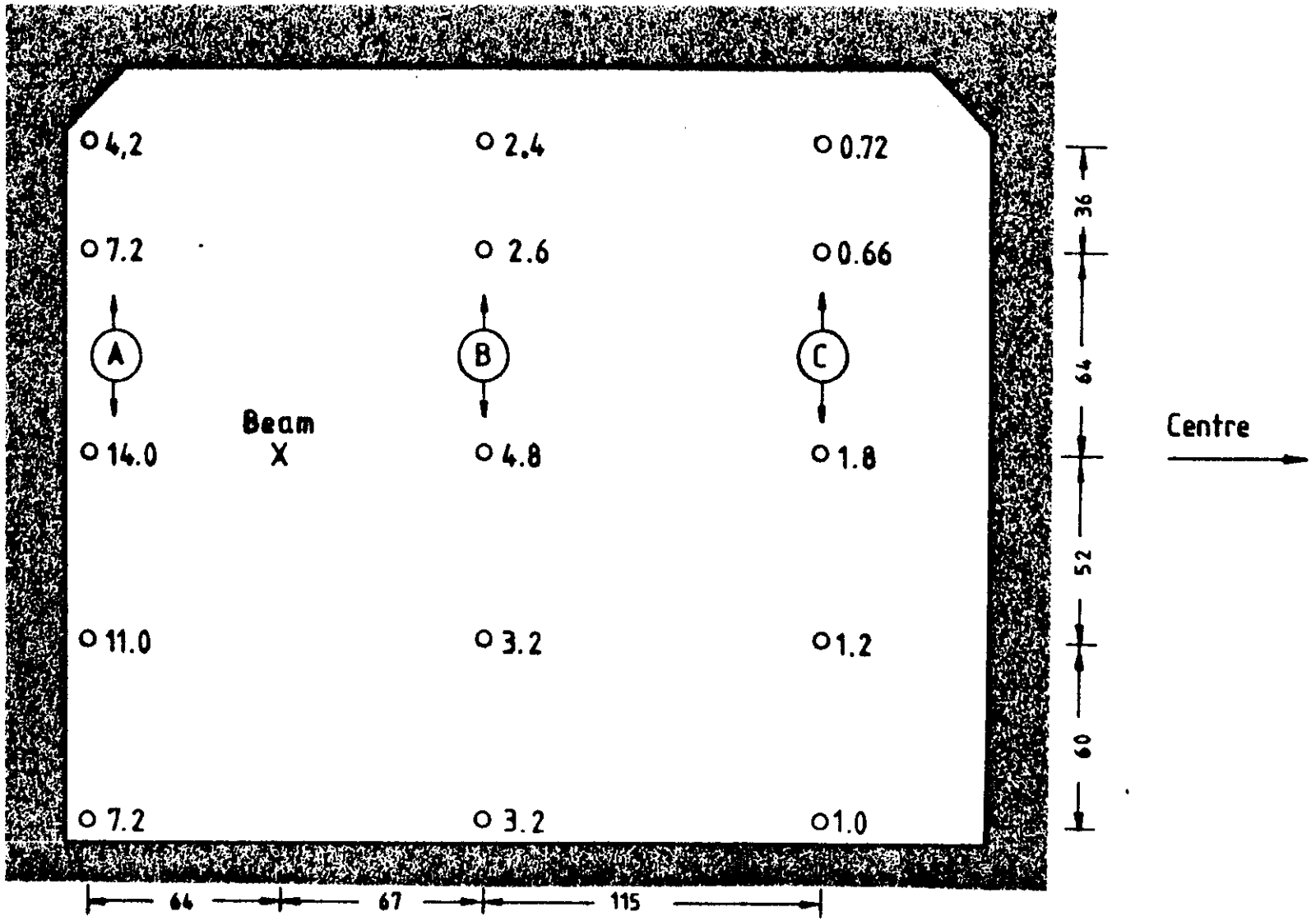

Units:
Distances : cm
Doses : 10^3 rad / 100 mAh

Fig.5

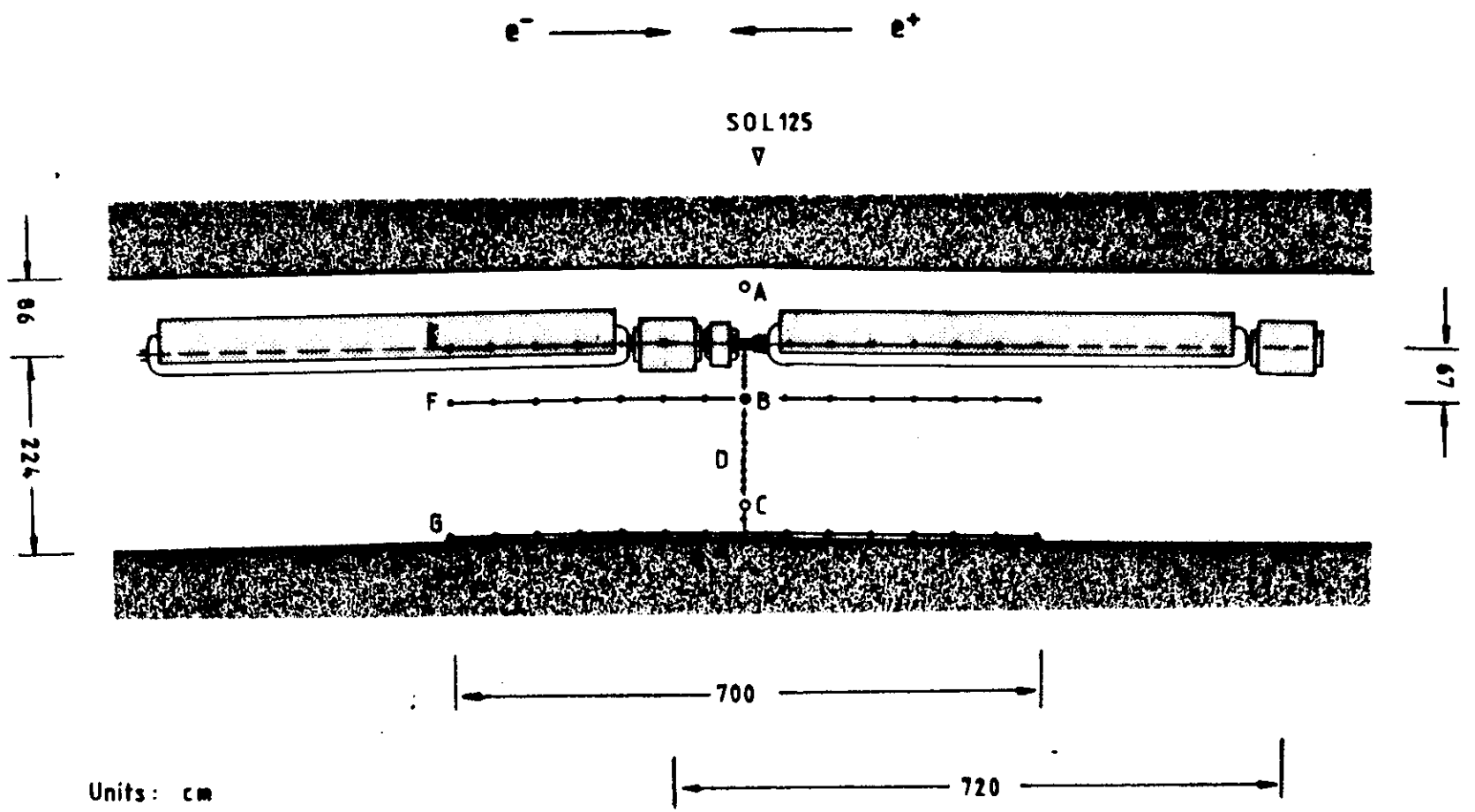

Fig.6

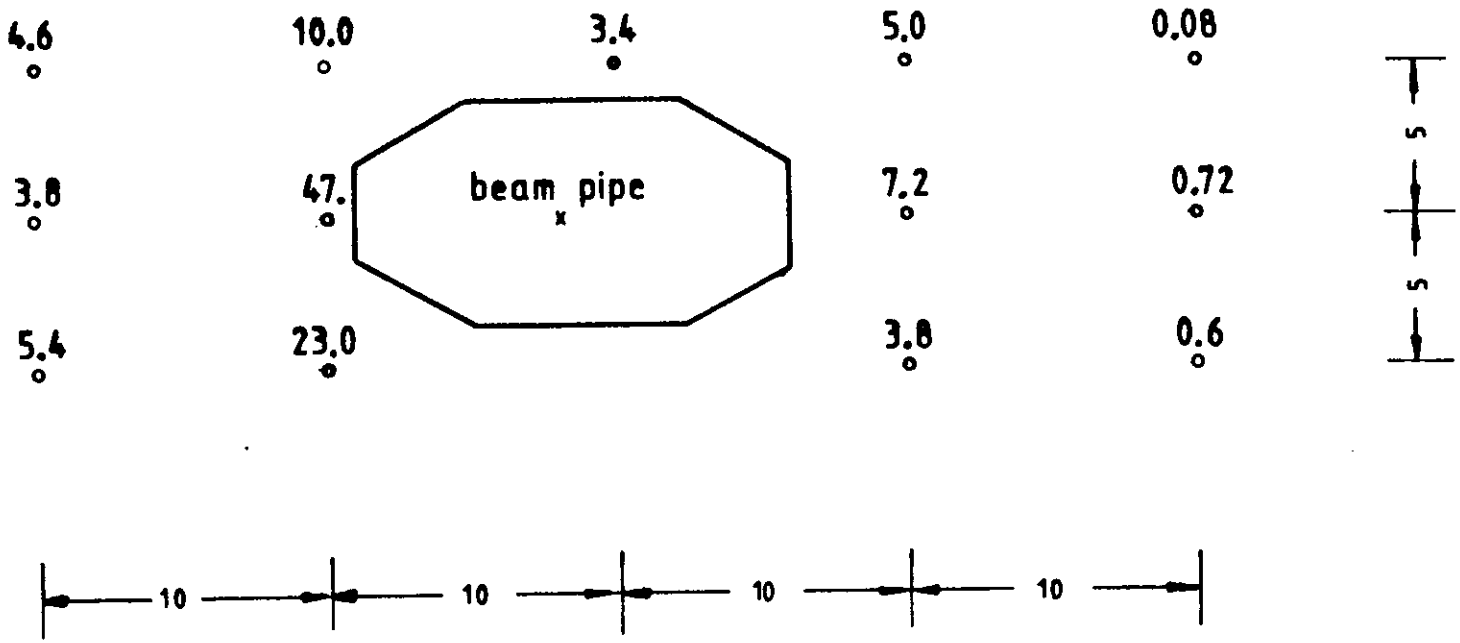

Centre

Units:
Distances: cm
Doses: 10^5 rad / 100 mAh

Fig. 7

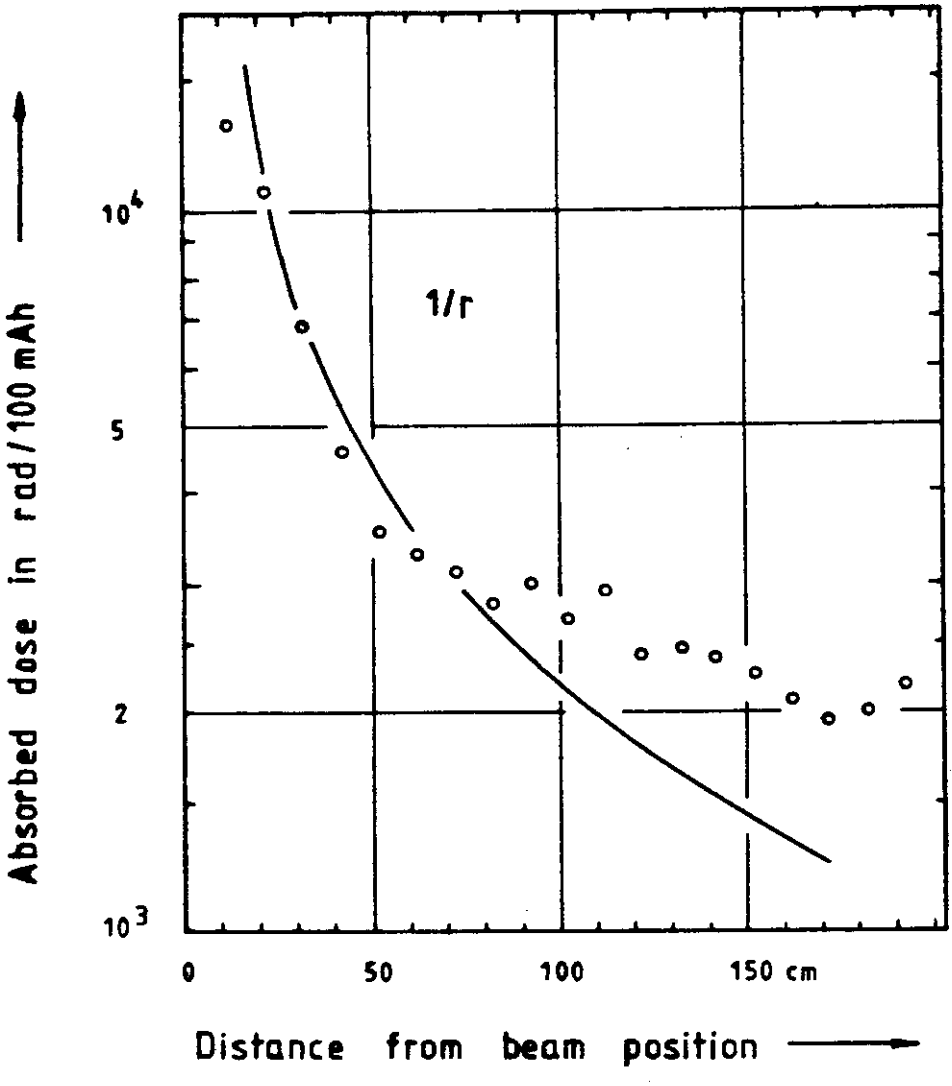
Absorbed dose in rad/100 mAh
10^4
5
2
10^3
1/r
0
50
100
150 cm
Distance from beam position

Fig. 8

PETRA Tunnel near SOL 125

(side-view)

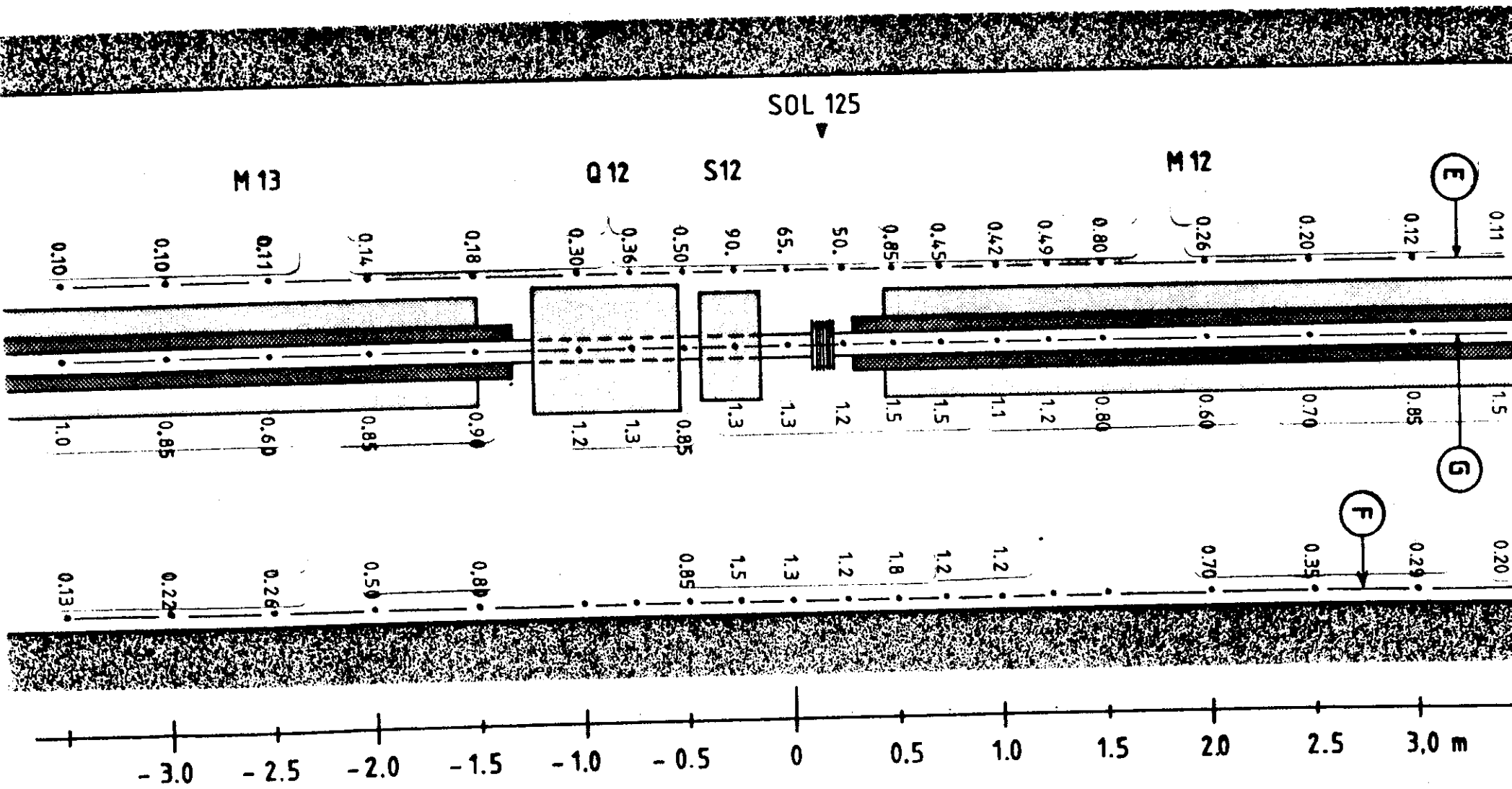

Units: 10^3 rad / 100 mAh

Fig.9

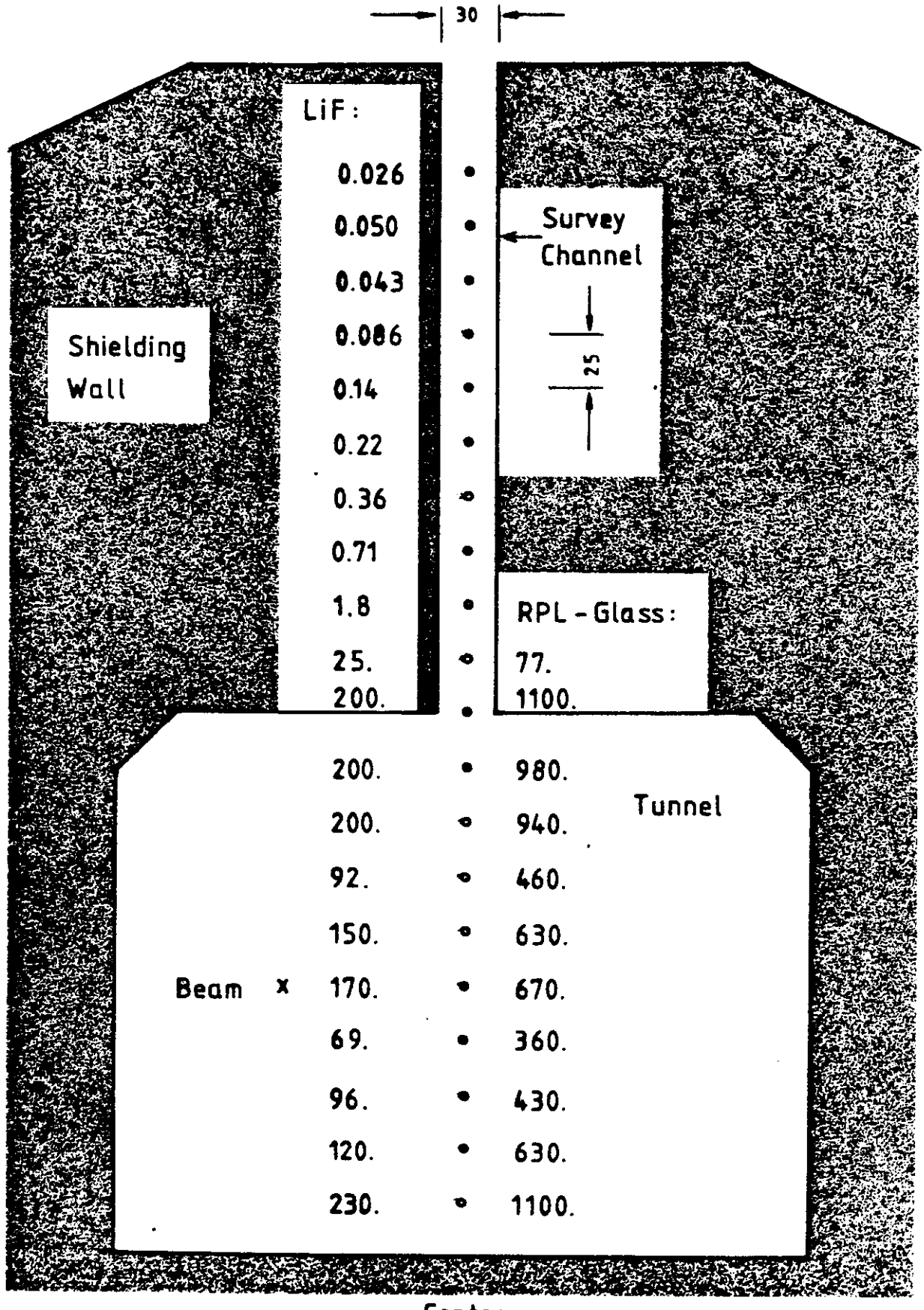

Units:
Distances : cm
Doses : rad / 100 mAh

Fig. 10